

## Coupling between the ferroelectric and antiferromagnetic orders in $\text{YMnO}_3$

Z. J. Huang, Y. Cao, Y. Y. Sun, Y. Y. Xue, and C. W. Chu

*Department of Physics and Texas Center for Superconductivity, University of Houston, Houston, Texas 77204-5932*

(Received 26 March 1997)

Anomalies in the dielectric constant and loss tangent have been observed in the ferroelectromagnet  $\text{YMnO}_3$  near its Néel temperature of  $\sim 80$  K and below its ferroelectric Curie temperature of  $\sim 914$  K. These anomalies are indicative of coupling between the ferroelectric and antiferromagnetic orders in this compound. A small but distinct magnetoelectric effect and a magnetoresistive effect up to  $\sim 15\%$  were also detected in a magnetic field at 5 T. The results will be contrasted with previous theoretical predictions.

[S0163-1829(97)00430-X]

The yttrium and rare-earth manganites  $\text{RMnO}_3$  crystallize in two structural phases:<sup>1,2</sup> The hexagonal phase for  $R=\text{Ho, Er, Tm, Yb, Lu, or Y}$ , which has a small ionic radius, and the orthorhombic phase for  $R=\text{La, Ce, Pr, Nd, Sm, Eu, Gd, Tb, or Dy}$ , which possesses a greater ionic radius. In these compounds, the angle Mn-O-Mn is close to  $180^\circ$ , facilitating magnetic ordering via an indirect exchange interaction between the Mn ions through the O ions. While magnetic ordering occurs in both hexagonal and orthorhombic manganites,<sup>3</sup> ferroelectric ordering occurs only in the hexagonal,<sup>1</sup> which belong to the noncentrosymmetric  $P6_3cm$  space group. Therefore, the hexagonal yttrium and rare-earth manganites form an interesting class of materials known as ferroelectromagnets<sup>4</sup> in which the ferroelectric and magnetic orders coexist at low temperatures. The study of ferroelectromagnets may offer insights into the occurrence of ferroelectricity and magnetism in these and related oxides by examining the coupling between the two orders. This coupling can result in the so-called magnetoelectric effect with an interesting device potential, where the dielectric (magnetic) properties of the ferroelectromagnets may be altered by the onset of the magnetic (electric) transition or by the application of a magnetic (electric) field. The recent discovery<sup>5</sup> of colossal magnetoresistance in doped  $\text{LaMnO}_3$  near its magnetic transition temperature provides added interest to the study of manganites.

Experiments were carried out on ferroelectromagnets,<sup>4</sup> mostly in the 1960s and 1970s, by scientists in the former Soviet Union. Evidence for coupling between the ferroelectric and magnetic orders and for magnetoelectric effect has been reported. Many of the compounds examined were with complex compositions,<sup>6</sup> i.e., having ions of different valence (or magnetic nature) in the octahedral positions or with two very similar transition temperatures.<sup>7</sup> The observations were explained qualitatively in terms of models<sup>8</sup> based on the Landau theory of phase transitions by assuming the ferroelectric ordering temperature ( $T_E$ ) to be very close to the magnetic ordering temperature ( $T_M$ ). Intuitively, the coupling effect may diminish as the difference between  $T_E$  and  $T_M$  increases. Thus the existence of such a coupling may not be self-evident for ferroelectromagnets with  $T_E$ 's very different from their  $T_M$ 's. Although a maximum in the dielectric constant ( $\epsilon$ ) of the ferroelectromagnet  $\text{BiFeO}_3$  near and above the antiferromagnetic  $T_M \sim 643$  K, but way below its ferro-

electric  $T_E \sim 1023$  K, has been taken as evidence for the coupling between the two orders,<sup>9</sup> the increasingly large electrical conductivity near and above  $T_M$  of this compound cannot be ruled out unambiguously as the cause for the  $\epsilon$  anomaly. Therefore, we have decided to search for evidence of coupling between the ferroelectric and magnetic orders in hexagonal  $\text{YMnO}_3$ ,<sup>10</sup> which displays a ferroelectric  $T_E \sim 914$  K, but a rather low antiferromagnetic  $T_M \sim 80$  K, and has a resistivity ( $\rho$ )  $> 10^{11}$   $\Omega$  cm at  $T_M$ . We have measured the dielectric and magnetic properties as a function of temperature both in the absence and in the presence of a magnetic field. An inverse S-shaped anomaly in both  $\epsilon$  and loss tangent ( $\tan\delta$ ) has been detected near  $T_M$ , indicative of coupling between the two orders. A small but distinctive magnetoelectric effect was detected in the presence of a 5-T field, as evidenced by a slight suppression of both  $\epsilon$  and  $\tan\delta$  near  $T_M$ . A negative magnetoresistive effect increasing with cooling up to 15% was also observed at  $\sim 230$  K, below which  $\rho > 2 \times 10^{11}$   $\Omega$  cm becomes too large for us to measure. While the  $\epsilon$  anomaly detected is expected when the ferroelectric and magnetic orders interact, the shape of the  $\epsilon$  and  $\tan\delta$  anomalies is rather different from that predicted.<sup>8</sup>

The samples investigated were prepared by the solid-state reaction technique at ambient pressure. Cation oxides  $\text{Y}_2\text{O}_3$  (99.99%) and  $\text{MnO}_2$  (99.99%) were thoroughly mixed in a ratio of 1:2 to achieve the cation stoichiometry of  $\text{YMnO}_3$ . They were then compacted and calcinated in air at  $1100^\circ\text{C}$  for 13 h. The reacted product was ground, compacted, and reheated at  $1100^\circ\text{C}$  for 12 h to ensure its homogeneity. The resulting pellets were not dense enough for our dielectric measurements. They were subsequently pulverized, compressed, and sintered at  $\sim 1300^\circ\text{C}$  for  $\sim 12$  h to achieve improved compaction. These relatively dense pellets were then cut into bars or disks for study. The structure was determined by powder x-ray diffraction (XRD), employing a Rigaku D-MAX/BIII diffractometer. The  $\epsilon$ ,  $\tan\delta$ , and  $\rho$  were determined using a HP-4262A LCR meter at frequencies of 120 Hz to 10 kHz, and a HP-4285A precision LCR meter at frequencies of 75 kHz to 30 MHz. The polarization–electric-field ( $P$ - $E$ ) hysteresis loop was measured using the standard Sawyer-Tower method operated at 2.61 kHz, using a HP 54502A digital oscilloscope. The magnetic susceptibility ( $\chi$ ) was determined by a Quantum Design (SQUID) magnetometer.

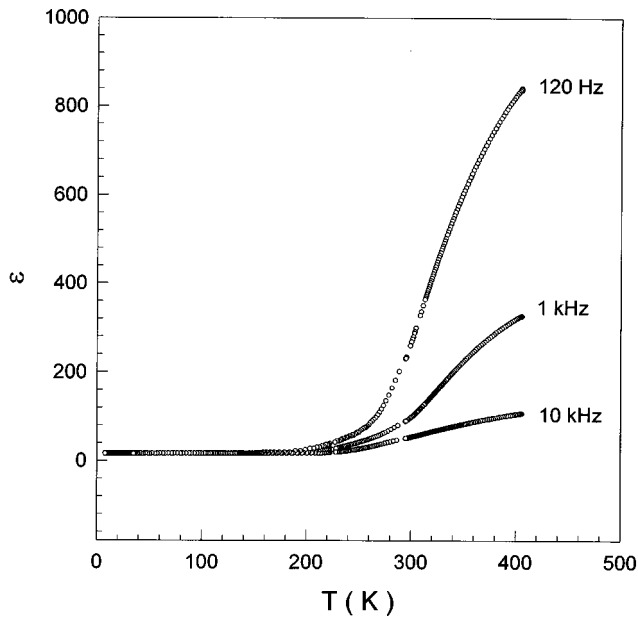


FIG. 1. Temperature dependence of the dielectric constant ( $\epsilon$ ) at different frequencies.

The XRD results show that the sample is pure with a single hexagonal  $\text{YMnO}_3$  phase within its resolution of  $\sim 3\%$ . The lattice parameters are  $a=6.13 \text{ \AA}$  and  $c=11.4 \text{ \AA}$ , in agreement with previous reports.<sup>2</sup> No sign of  $\text{Mn}_2\text{O}_3$ , which usually forms at synthesis temperatures above  $1200 \text{ }^\circ\text{C}$ , or orthorhombic  $\text{YMnO}_3$ , which appears at high pressures, was detected. However, the density of the samples was still low, i.e.,  $\sim 80\%$ , in spite of our  $1300 \text{ }^\circ\text{C}$  sintering. As a result, certain uncertainties in the numerical values of  $\epsilon$ ,  $\tan\delta$ , and  $P$  are to be expected, but will not affect the conclusions to be drawn.

The temperature dependence of  $\epsilon$  of  $\text{YMnO}_3$  is shown in Fig. 1 for three different frequencies. A rapid rise of  $\epsilon$  above  $\sim 200$  to  $\sim 400 \text{ K}$ , the highest temperature of our experiment, is clearly evident, consistent with a  $T_E$  above  $400 \text{ K}$ , previously reported.<sup>1</sup> The  $P$ - $E$  hysteresis was easily observed at  $300 \text{ K}$ , showing a ferroelectric ground state for  $\text{YMnO}_3$  at this temperature. Here  $\chi(T)$  is small and shows a Curie-Weiss behavior above  $\sim 100 \text{ K}$ , with a paramagnetic Curie temperature of  $\sim 510 \text{ K}$ , as displayed in Fig. 2. The  $\chi(T)$  results at  $1 \text{ T}$  are in agreement with previous reports.<sup>3</sup> There is no direct  $\chi$  anomaly in the temperature range investigated in this study, although an antiferromagnetic transition at  $T_M \sim 80 \text{ K}$  was observed in both the Mössbauer experiments<sup>11</sup> and neutron-diffraction experiments. As was pointed out<sup>12</sup> previously, the antiferromagnetic transition in  $\text{YMnO}_3$  does not lead to any anomaly of the temperature dependence of the magnetic susceptibility. A similar situation is also true in the cases of  $\text{Nb}_2\text{Co}_4\text{O}_9$  (Ref. 13) and  $\text{PrBa}_2\text{Cu}_3\text{O}_7$  (Ref. 14). In an attempt to look for an anomaly in the magnetic properties due to the antiferromagnetic transition, we plotted  $d\chi(T)/dT$  vs  $T$  in Fig. 3. It clearly shows an anomaly near the antiferromagnetic  $T_M \sim 80 \text{ K}$ , similar to several other antiferromagnetic oxide systems including  $\text{PrBa}_2\text{Cu}_3\text{O}_7$ .<sup>14</sup> The anomaly is thus used to define the transition in these oxides, which is in good agreement with the results of neutron-diffraction and specific-heat experiments.

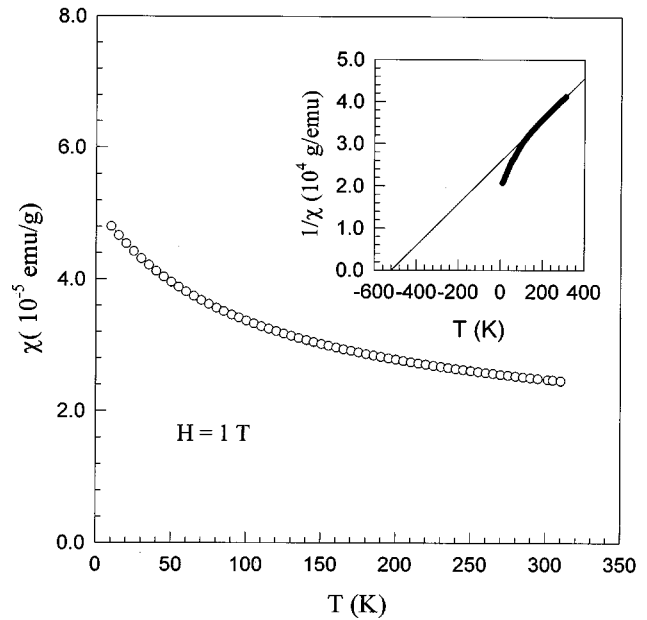


FIG. 2. Temperature dependence of the dc magnetic susceptibility ( $\chi$ ) at  $1 \text{ T}$ . Inset:  $1/\chi$ .

Measurements of  $\epsilon$  and  $\tan\delta$  were carried out near  $T_M \sim 80 \text{ K}$  with higher precision to determine if coupling between the ferroelectric and antiferromagnetic orders exist. The results are shown in Figs. 4 and 5. As clearly apparent in the insets of those figures, an inverse-S-shaped anomaly similar to that in  $d\chi/dT$  was detected in  $\epsilon$  and  $\tan\delta$  as  $\text{YMnO}_3$  entered its antiferromagnetic state, indicating a coupling between the two orders. On the application of a magnetic field of  $5 \text{ T}$ , both  $\epsilon$  and  $\tan\delta$  are depressed near  $T_M$  and the  $\tan\delta$  depression continues to  $\sim 15 \text{ K}$ , the lowest temperature of our experiment, while the inverse-S-shaped anomalies of  $\epsilon$  and  $\tan\delta$  have shifted slightly to higher temperatures. Consequently, the general magnetoelectric effect

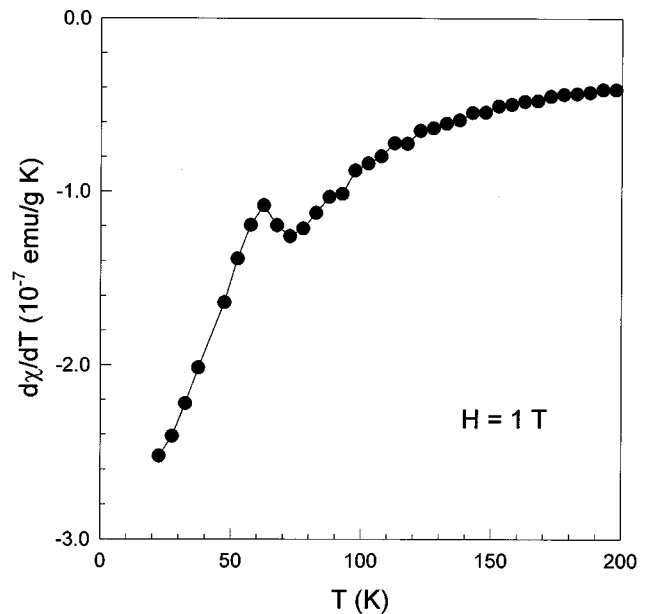


FIG. 3. Temperature dependence of the derivative of the dc magnetic susceptibility ( $d\chi/dT$ ) at  $1 \text{ T}$ .

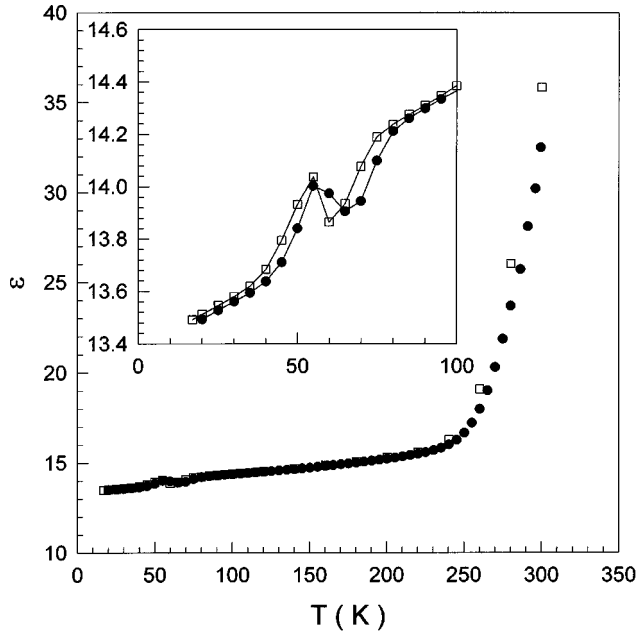


FIG. 4.  $\varepsilon(T)$  at 75 kHz near  $T_M$  at ( $\square$ ) 0 T and ( $\bullet$ ) 5 T.

predicted<sup>4,8</sup> in a ferroelectromagnet was observed in  $\text{YMnO}_3$ .

The dc  $\rho$  was found to increase exponentially as temperature decreases, as shown in Fig. 6. In the presence of a 5-T magnetic field, a negative magnetoresistance was observed below  $\sim 260$  K with an increasing magnitude to  $\sim 15\%$  near 230 K, as displayed in the inset.

In the absence of an externally applied magnetic or electric field, the ferroelectric and magnetic orders in a ferroelectromagnet may couple via an electron-phonon interaction.<sup>9,10</sup> For instance, the ferroelectric properties may alter the onset of a magnetic transition, arising from a change of the charge configuration associated with an exchange-field change accompanying the magnetic order. On the other hand, the mag-

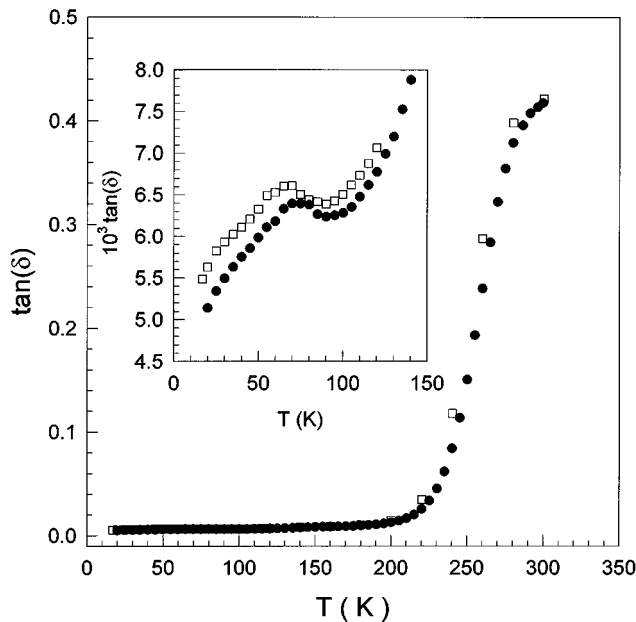


FIG. 5.  $\tan\delta(T)$  at 75 kHz near  $T_M$  at ( $\square$ ) 0 T and ( $\bullet$ ) 5 T.

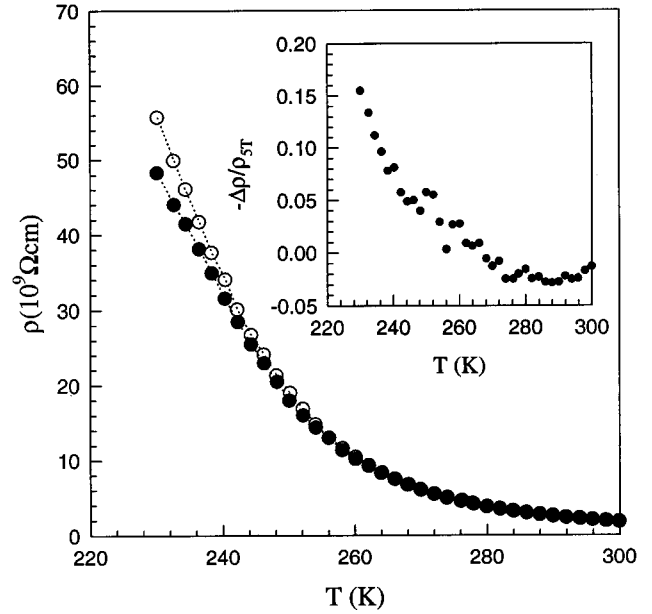


FIG. 6. Temperature dependence of resistivity ( $\rho$ ) at ( $\circ$ ) 0 T and ( $\bullet$ ) 5 T. Inset: the temperature dependence of magnetoresistivity  $-\Delta\rho/\rho_{5T}$ .

netic properties may vary with the onset of a ferroelectric transition resulting from a change of spin configuration associated with the lattice change accompanying the ferroelectric order. Phenomenologically, the coupling between the ferroelectric and ferromagnetic orders can be described by an electromagnetic susceptibility tensor  $X$ ,

$$X = \begin{bmatrix} \hat{X}^{ee} & \hat{X}^{em} \\ \hat{X}^{me} & \hat{X}^{mm} \end{bmatrix},$$

where the tensor elements are related to the polarization ( $\vec{P}$ ) and the magnetization ( $\vec{M}$ ) vectors with their measuring electric ( $\vec{E}$ ) and magnetic ( $\vec{H}$ ) fields:

$$\vec{P} = \hat{X}^{ee}\vec{E} + \hat{X}^{em}\vec{H} \quad \text{and} \quad \vec{M} = \hat{X}^{me}\vec{E} + \hat{X}^{mm}\vec{H}.$$

It is evident that the off-diagonal tensors ( $\hat{X}^{me} = \hat{X}^{em}$ ) provide the coupling. It was later shown<sup>8</sup> that  $(\hat{x}^{me})^2 \ll \hat{X}^{ee}\hat{X}^{mm}$ , implying a larger magnetoelectric effect for ferroelectromagnets. By assuming that  $T_E$  and  $T_M$  are sufficiently close, it was found<sup>8</sup> that there is a smooth change in the temperature dependence of  $\hat{X}^{ee}(\hat{X}^{mm})$  at the ferromagnetic (ferroelectric) transition. The inverse-S-shaped anomaly observed in  $\varepsilon$ , which is proportional to  $\hat{X}^{ee}$  shown in the inset of Fig. 4, is in clear contrast with that predicted for a ferroelectroferromagnet.<sup>8</sup> Given the overall  $M=0$  for an antiferromagnet, the magnetoelectric effect observed in the absence of an external field is very likely a result of a magnetorestrictive effect associated with a lattice change accompanying the Néel transition. This can give rise to a step change in  $P$ , and the temperature derivative of  $P$  will have an inverse-S-shaped anomaly observed in  $\varepsilon$  and  $\tan\delta$ . The continued shift of  $\tan\delta$  below  $T_M$  may be the result of the negative magnetoresistance observed, as shown in Fig. 6. Detailed x-ray-diffraction experiments are under way. The theoretical model for a ferroelectric antiferromagnet such as

YMnO<sub>3</sub> is more complicated, since one has to treat the two magnetic sublattices in this material separately. A model of a second-order phase transition based on Landau theory is being developed to account for the observation.

A rich phase diagram for a ferroelectric antiferromagnet with coupling between the two orders in an external magnetic field has been developed, and the magnitude of the magnetic (electric) field effect on  $\vec{P}(\vec{M})$  for a ferroelectric antiferromagnet has been calculated.<sup>4</sup> Unfortunately, a meaningful comparison between the observation and the prediction can only be made when better data from single-crystal samples are obtained. The shift of the anomalies in  $\epsilon$  and  $\tan\delta$  toward higher temperature may simply be accounted for as a magnetic-field-enhanced Néel transition sometimes observed in an antiferromagnet. The reason for the relatively large magnetoresistance effect is unknown, although it is consistent with results recently reported<sup>15</sup> on the colossal magnetoresistor Y-doped (La,Ca)MnO<sub>3</sub>.

In summary, we have observed anomalies in  $\epsilon$  and  $\tan\delta$  in YMnO<sub>3</sub> with a ferroelectric temperature of 914 K as it enters

its antiferromagnetic state near 80 K, indicative of a coupling between the ferroelectric and magnetic order, in spite of the large difference between the two ordering temperatures. This is attributable to a change in the phonon spectrum of YMnO<sub>3</sub> associated with the antiferromagnetic transition via a possible magnetostrictive effect. The upward shift of the  $\epsilon$  and  $\tan\delta$  anomalies near  $T_M$  by an external magnetic field to higher temperature may be a result of the magnetic field effect on the antiferromagnetic transition. The magnetoresistive effect observed is unknown, although this stems from the same reason for the colossal magnetoresistance in Y-doped (La,Ca)MnO<sub>3</sub> previously observed. This effect may account for the constant shift of  $\tan\delta$  by field at low temperature, providing a control on the dielectric properties of a ferroelectric without contact electrodes.

The work in Houston is supported in part by NSF Grant No. DMR 95-00625, the T.L.L. Temple Foundation, the John J. and Rebecca Moores Endowment, and the State of Texas through the Texas Center for Superconductivity at the University of Houston.

<sup>1</sup>F. Bertant, F. Forrat, and P. Fang, C. R. Acad. Sci. **256**, 1958 (1963).

<sup>2</sup>H. L. Yakel, W. C. Koehler, E. F. Bertant, and E. F. Forrat, Acta Crystallogr. **16**, 957 (1963).

<sup>3</sup>W. C. Koehler, H. L. Yakel, E. O. Wollan, and J. W. Cable, Phys. Lett. **9**, 93 (1964); R. Pauthenet and C. Veyret, J. Phys. (France) **31**, 65 (1970); V. E. Wood, A. E. Austin, E. W. Collings, and K. C. Brog, J. Phys. Chem. Solids **34**, 857 (1973).

<sup>4</sup>For a review, see G. A. Smolenskii and I. E. Chupis, Sov. Phys. Usp. **25**, 475 (1982).

<sup>5</sup>R. von Helmolt, J. Wecker, B. Holzapfel, L. Schultz, and K. Samwer, Phys. Rev. Lett. **71**, 2331 (1993); S. Jim, T. H. Tiefel, M. McCormack, R. A. Fastnacht, R. Mamesh, and L. H. Chen, Science **264**, 413 (1994).

<sup>6</sup>See, for example, V. A. Bokov, I. E. Myl'nikova, and G. A. Smolenskii, Sov. Phys. JETP **15**, 447 (1962).

<sup>7</sup>See, for example, E. Ascher, H. Rieder, H. Schmid, and H.

Stossel, J. Appl. Phys. **37**, 1404 (1966).

<sup>8</sup>G. A. Smolenskii, Sov. Phys. Solid State **4**, 807 (1962); G. M. Nedlin, *ibid.* **4**, 2612 (1963).

<sup>9</sup>Y. Y. Tomashpol'skii, Y. N. Venetsev, and G. S. Zhdanov, Sov. Phys. JETP **19**, 1294 (1964).

<sup>10</sup>G. A. Smolenskii and V. A. Bokov, J. Appl. Phys. **35**, 915 (1964).

<sup>11</sup>J. Chappert, Phys. Lett. **18**, 229 (1965).

<sup>12</sup>S. A. Kizhaev, V. A. Bokov, and O. V. Kachalov, Sov. Phys. Solid State **8**, 215 (1966).

<sup>13</sup>E. F. Bertaut, L. Corliss, F. Forrat, R. Aleonard, and R. Pauthenet, J. Phys. Chem. Solids **21**, 234 (1961).

<sup>14</sup>A. Kebede, C. S. Jee, J. Schwegler, J. E. Crow, T. Mihalisin, G. H. Myer, R. E. Salomon, P. Schlottmann, M. V. Kuric, S. H. Bloom, and R. P. Guertin, Phys. Rev. B **40**, 4453 (1989).

<sup>15</sup>H. Y. Hwang, S. W. Cheong, P. G. Radaelli, M. Marezio, and B. Batlogg, Phys. Rev. Lett. **75**, 914 (1995).